Long-term dust climatology in the western United States reconstructed from routine aerosol ground monitoring

Daniel Q. Tong[1,2*], Mo Dan[1,3*], Tong Wang[3], Pius Lee[1]

1. US National Oceanic and Atmospheric Administration (NOAA), Air Resources Laboratory, Silver Spring, MD 20910 USA
2. Northeastern Institute of Geography and Agroecology, Chinese Academy of Sciences, Changchun, China
3. Beijing Municipal Institute of Labor Protection, Beijing, China

* Contact Information (DQT and MD): NOAA/OAR/ARL
1315 East West Highway, Silver Spring, MD 20910 USA
Email: daniel.tong@noaa.gov (DQT); danmo2001@gmail.com (MD)
Voice: 301-713-0295 ext 101 Fax: 301-713-0119

For submission to: **Atmospheric Chemistry and Physics**

Abstract:

This study introduces an observation-based dust identification approach and applies this method to reconstruct long-term dust climatology in the western United States.Long-term dust climatology is important for quantifying the effects of atmospheric aerosols on regional and global climate. Although there exist many routine aerosol monitoring networks, it is often difficult to obtain dust records from these networks, because these monitors are either deployed far away from dust active regions (most likely collocated with dense population) or contaminated by anthropogenic sources and other natural sources, such as wildfires and vegetation detritus. Here we propose an approach to identify local dust events relying solely on aerosol mass and composition from general-purpose aerosol measurements. Through analyzing the chemical and physical characteristics of aerosol observations during satellite-detected dust episodes, we select five indicators to be used to identify local dust records: 1) high PM_{10} concentrations; 2) low $PM_{2.5}/PM_{10}$ ratio; 3) higher concentrations and percentage of crustal elements; 4) lower percentage of anthropogenic pollutants; and 5) low enrichment factors of anthropogenic elements. After establishing these identification criteria, we conduct hierarchical cluster analysis for all validated aerosol measurement data over 68 IMPROVE sites in the western United States. A total of 182 local dust events were identified over 30 of the 68 locations from 2000 to 2007. These locations are either close to the four U.S. Deserts, namely the Great Basin Desert, the Mojave Desert, the Sonoran Desert, and the Chihuahuan Desert, or in the high wind power region (Colorado). During the eight-year study period, the total number of dust events displays an interesting four-year activity cycle (one in 2000-2003 and the other in 2004-2007). The years of 2003, 2002 and 2007 are the three most active dust periods, with 46, 31 and 24 recorded dust events, respectively, while the years of 2000, 2004 and 2005 are the calmest periods, all with single digit dust records. Among these deserts, the Chihuahuan Desert (59 cases) and the Sonoran Desert (62 cases) are by far the most active source regions. In general, the Chihuahuan Desert dominates dust activities in the first half of the eight-year period while the Sonoran Desert in the second half. The monthly frequency of dust events shows a peak from March to July and a second peak in autumn from September to November. The large quantity of dust events occurring in summertime also suggests the prevailing impact of windblown dust across the year. This seasonal variation is consistent with previous model simulations over the United States.

Keywords: Dust, aerosols, climatology, air quality, IMPROVE, drought

Introduction

Due to its various effects on air quality and climate (Intergovernment Panel on Climate Change, IPCC, 2007), dust aerosol lifted from disturbed soil has been extensively studied through ground observation, remote sensing and model simulations (Gillette and Passi, 1988; Gong et al., 2003; Reid et al., 2003; Zhang et al., 2003). For both remote sensing and modeling studies, ground measurements are critically important for verifying derived results. Specific ground-based monitoring networks have been established to facilitate dust detection (Zhang et al., 2003) and to assist in calibrating and improving aerosol models (Gong et al., 2003). In most cases, however, ground aerosol monitoring networks are deployed for other purposes, such as monitoring visibility (Pitchford and Malm, 1994) and protecting human health (Bell et al., 2007). Therefore, it is difficult to utilize these monitors to identify dust events because the monitoring sites are either deployed far away from dust active regions (most likely collocated with dense population) or contaminated by anthropogenic sources. Even at rural or background sites, other natural sources, such as wildfires and vegetation detritus, and long-range transported dust can contribute to monitor readings (e.g., Edgerton et al., 2009; Jaffe et al., 2004). Consequently, it is difficult to directly utilize the measurement data from such monitoring networks to detect dust from local sources or to assess dust model performance. The regulatory monitoring networks, however, represent the majority of air quality monitoring around the world. The incapability of utilizing such a large set of data results is a missed opportunity to gain insight into dust activities from the perspective of "ground truth".

A myriad of observation-based methods have been proposed to identify dust events using satellite observation, computer models and ground and laboratory measurements. These methods vary in complexity and applicability, but in general fall into three categories: laboratory-based approach, and remote sensing-based approach and ground monitor-based approach. In the early years, radioative elements, such as Radon-222, have been used as a tracer of dust transport from Africa (Prospero, 1970). In later studies, the mineral dust component in sampled aerosols was determined by the weight of ash residue from the high-temperature burning of sampling filter after being extracted with deionized water (Prospero, 1999). Another laboratory study differentiated dust particles from other types of transportable particles collected on board the NOAA Research Vessel Ronald H. Brown through individual-particle analysis using an

automated scanning electron microscope (SEM) and a field emission scanning electron microscope (FESEM) (Gao et al., 2007).

With the rapid expansion of remote sensing data, several studies have attempted to detect dust outbreaks using satellite images and other derived products (Kauffman et al., 2000; Prospero et al, 2002; Rivera-Rivera et al., 2010; Lee et al, 2009). The pioneer works by Prospero and colleagues have associated dust sources with barren areas with "depressed" elevations relative to their surroundings (Ginoux et al., 2001) based on satellite-based global observations from the NIMBUS 7 Total Ozone Mapping Spectrometer (TOMS) (Prospero et al., 2002). They found that the major dust sources are invariably associated with topographical lows in arid or semiarid regions with rainfall below 250 mm (Prospero et al., 2002). A recent work by Ginoux et al (2010) combines land use data with the Moderate Resolution Imaging Spectroradiometer (MODIS) Deep Blue algorithm to identify natural and anthropogenic dust sources over the western Africa. This approach is further developed to pin-point active dust sources in the North America by selecting grid cells based on the frequency of high aerosol optical depth (AOD) events (AOD = 0.75) (Draxler et al., 2010). In an effort to quantify the relative impacts of Saharan and local dust in Elche in Southeastern Spain, Nicolas et al. (2008) combined satellite images from the NASA SeaWiFS, two dust prediction models (NAAPS and DREAM), a back-trajectory model (HYSPLIT) and NCEP meteorological reanalysis data to detect the outbreaks of African dust events. Using Positive Matrix Factorization (PMF), they identified six PM_{10} sources, including local soil and African dust, which are distinguished by the correlation of the source intensity with Ti. In Asia, an operational dust retrieval algorithm has been developed based on the FY-2C/SVISSR through combining visible and water vapor bands observations of the geostationary imager to distinguish dust plumes from surface objects and clouds (Hu et al., 2008). In the United States, data from both polar-orbiting and geostationary satellites have been used to characterize source areas of large dust outbreaks (Lee et al., 2009; Rivera-Rivera et al., 2010). It should be mentioned that all of these dust source identification methods are based on satellite remote sensing that needs to be independently verified using ground observations. For instance, Schepanski et al. (2007, 2012) combined a back-tracking method with high temporal satellite aerosol data (15-min Aerosol Index (AI) from the Ozone Monitoring Instrument (OMI)) to identify dust sources over the Saharan region. They found that the spatial distribution of dust

source areas inferred from OMI 15-min AI is distinctly different from that by using the daily MODIS Deep Blue aerosol data (Schepanski et al., 2012).

Beside these laboratory and remote sensing studies, dust identification methods have also been developed based exclusively on aerosol mass concentration and its correlation with meteorological conditions. Kavouras and co-workers (2007) developed a semi-quantitative method to assess local dust contribution in the western United States utilizing multivariate linear regression of dust concentrations against categorized wind parameters. In their study, dust concentrations are assumed equal to the sum of fine soil and coarse particles using an operational definition adopted from Malm et al. (1994, 2000a, 2000b). Escudero et al. (2007) proposed a method to quantify the daily African dust load by subtracting the daily regional background level from the PM_{10} concentration value. Ganor et al (2009) developed and tested an automated dust identification algorithm for monitoring location in Israel. Their algorithm determined a dust event by three conditions: half-hour PM_{10} average level exceeds 100 $\mu g/m^3$, this high level maintained for at least three hours, and the peak PM_{10} ever reaches 180 $\mu g/m^3$. In most aerosol observations, however, the dust emission conditions or visual identification information are not available. Consequently, it is challenging to identify local windblown dust events based on particle concentration or chemical species because of the variability in meteorological conditions, dust strength and the distance from source areas (e.g. Luo et al. 2003).

We propose here a comprehensive dust identification approach and apply this method to reconstruct long-term dust climatology over the western United States. During local dust storms, air samples demonstrate distinct physical and chemical characteristics, “fingerprints” that can be used to pinpoint these events based on element abundance and size distribution. This ground-monitoring based method identifies individual local dust events using five dust indicators, including mass concentrations, chemical composition and size distribution. These indicators are chosen from case studies of the aerosol data collected during three large dust storms identified independently by satellite remote sensing. Some of these indicators are being used in previous dust identification works. We demonstrate here that the concurrent application of all five criteria lends greater confidence to the reconstructed dust dataset in the absence of other complementary measures. Hierarchical cluster analysis is subsequently conducted to apply these indicators to daily aerosol data, so that a group of local dust aerosol samples that best matches these identification criteria can be separated from other aerosols of other origins. The use of cluster

analysis not only allows us to process large dataset, but also provides identifying threshold values through clustering all aerosol data based on their statistical similarity in physical and chemical characteristics. In addition, we apply this approach to scan the IMPROVE data from 2000 to 2007, and identify 182 local dust samples over 30 locations in the western United States. A dataset of identified local dust events provide useful information for regulators to pinpoint natural dust events and for researchers to verify remote sensing products and atmospheric modeling results. In addition, the detailed chemical data collected during these identified dust events make it possible to determine the chemical composition of dust aerosols. The representation of chemically speciated dust aerosols allows atmospheric modeler to directly compare model predicted crustal and trace elements with field measurements. Atmospheric modelers, when equipped with such information, will be able to explicitly simulate the concentrations and deposition of critical nutrients (e.g., Fe) and toxic elements to study the climate, health and biogeochemical effects of dust aerosols.

2. Methodology

2.1 Approach to identify local dust records

This approach consists of several consecutive steps. First, we review the satellite data from the MODIS sensors to identify well-recorded large dust events that originate within the United States. Based on the time and location of these satellite detected storms, we obtain the ground measurement data from the Interagency Monitoring of Protected Visual Environments (IMPROVE) network in the western United States. If there are valid IMPROVE measurements, these cases will serve as the dust "samples" to explore potential rules for identifying local dust aerosols. The second step of this approach is to examine the physical and chemical characteristics of the “known dust” samples. We are particularly interested in the following parameters: PM_{10} and $PM_{2.5}$ (particles smaller than 10 and 2.5 μm in diameter, respectively) mass concentrations, ratio of $PM_{2.5}$ to PM_{10}, percentage of crustal elements in $PM_{2.5}$, percentage of industrial, residential or biomass burning elements in $PM_{2.5}$, and enrichment factors of several crustal and anthropogenic elements.

The rationale behind choosing these parameters varies. In general, a dust event is associated with reduced visibility, resulting from increased levels of fine and coarse particles in the air (Malm et al., 1994). Therefore, $PM_{2.5}$ and PM_{10} concentrations during dust events are considerably higher than the typical levels. High PM concentrations, however, do not warrant a

local dust event. For instance, long-range transported Asian and African dust has been previously reported to cause air quality degradation in both the western and the eastern United States (Prospero, 1999; Jaffe et al., 2004; Fairlie, et al., 2007). To ensure the source of dust aerosols is local, we exclude the high PM data that is also associated with high $PM_{2.5}/PM_{10}$ ratio. Field and laboratory measurements of freshly emitted soil dust aerosols reveal a low $PM_{2.5}$ to PM_{10} ratio, which increases as dust plumes age. The US EPA uses a value of 0.15 - 0.26 for $PM_{2.5}$ to PM_{10} ratio for soil dust emissions from human activities (MRI, 2005). In this work, we remove the high PM data with the $PM_{2.5}/PM_{10}$ ratio higher than 0.35, considering these samples being contaminated with non-local dust sources. This ratio is chosen based on the emission splitting factors used fugitive dust particles by the US EPA (MRI, 2005), and previous field measurements of the $PM_{2.5}$ to PM_{10} ratio during dust events (e.g., 0.45 in Cheng, et al., 2005). Considering that most IMPROVE are not in the immediate proximity of dust source areas, we allow the cutoff ratio to be slightly larger (0.39) in the data processing. It should be noted that we consider all dust emissions from North America, including these from the Chihuahuan Desert in Mexico as local dust because the southern Chihuahuan Desert is a frequent dust source for aerosols in the southwestern US, especially Texas and New Mexico. The low $PM_{2.5}/PM_{10}$ ratio is also expected to exclude high PM concentration contributed by biomass burning, which is dominated by fine particles, resulting in a high $PM_{2.5}/PM_{10}$ ratio (Reid et al., 2005). A simple sensitivity test was conducted in the Discussion section to examine how sensitive the results are to the choice of the cutoff value.

Because dust particles can be mobilized by both wind erosion and human activities, we apply three additional criteria to distinguish windblown dust from anthropogenic fugitive dust or other intensive aerosol types (such as volcanic ash, wildfire, or vegetative detritus). Soil dust aerosols are associated with abundant crustal elements, which differentiate them from aerosols from biomass burning or fossil fuel combustion. This feature alone, however, can not distinguish natural dust from anthropogenic fugitive dust. In the United States, anthropogenic fugitive dust is the largest sector of primary PM emissions. The five major fugitive dust sources in the United States are vehicle emissions from unpaved road (47%), paved road (7%), agricultural operation (29%), and construction (11%), and mining/quarrying (7%). Each of these sources involves either fossil fuel combustion or other human activities in the immediate vicinity of dust sources. Therefore, compared to natural dust, anthropogenic dust aerosols contain higher anthropogenic-

originated elements, such as elemental carbon (from fossil fuel or biomass combustion) or heavy metals (such as Zn, Pd and Cu) from industrial operations (Chow et al., 1993; 2003; Reff et al., 2009). For instance, high levels of black carbon, Pb, Zn are found in paved road particles while high levels of nitrate (NO_3), Cr and Ni are found in unpaved road dust (Chow et al., 1993). Similarly, OC, K and Ca concentrations are high in animal husbandry dust and Ti, V, Mn concentrations in construction dust (Chow et al., 2003). Therefore, we use the concentrations and enrichment factors (EFs) of anthropogenic pollutants as the indicators to distinguish natural dust from anthropogenic dust. In this study, the enrichment factors (EFs) are calculated for a series of elements using Si as the reference element and the abundance of crustal elements at the Earth's surface as given by Taylor and McLennan (1985),

$$EF_X = \frac{(X/Si)_{aerosol}}{(X/Si)_{crustal}} \quad (1)$$

where $(X/Si)_{aerosol}$ and $(X/Si)_{crustal}$ represent the ratio of a certain species (X) to Si in sampled dust aerosols and in the Earth's surface soil, respectively. Species with EFs close to unity are considered to have a strong natural origin, while species with higher EFs have mainly an anthropogenic origin. By examining the variation of the above parameters, we can establish useful criteria for the subsequent statistical analysis to identify other local dust events that are not revealed by satellite data. Considering all the relevant parameters discussed above, five criteria will be the focus of subsequent statistical analysis: 1) PM_{10} and $PM_{2.5}$ concentrations; 2) Ratio of $PM_{2.5}$ to PM_{10}; 3) Concentrations of crustal elements Si, Ca, K, Fe, Ti; 4) Concentrations of anthropogenic pollutants, As, Zn, Cu, Pb, sulfate ,nitrate, Organic carbon (OC), and EC; and 5) enrichment factors (EF) of anthropogenic pollution elements Cu, Zn, Pb and K.

The third step of the procedure is to cluster all daily aerosol data according to these indicators, and to pinpoint a local dust group. This is achieved by applying hierarchical cluster analysis to IMPROVE daily data site by site for all selected sites. Cluster analysis is a statistical method that creates clusters of items or objects that have similarity within the same cluster but with differences between clusters. This technique has been previously applied to air quality studies to investigate source origins of air pollutants (e.g. Slanina et al., 1983; Dorling et al., 1992; Tong et al., 2005; Van Curen, et al., 2002). As discussed earlier, dust episodes are usually extraordinary events with large perturbations in both aerosol concentrations and chemical composition compared to that during non-dusty periods. Assuming spatial homogeneity in dust

chemical composition within a dust source region, we used the hierarchical cluster analysis to group all IMPROVE aerosol measurements based on the similarities in chemical and physical characteristics. The spatial homogeneity in dust composition, as observed in many desert regions, is likely due to the fact that the aerosol over the desert itself is well mixed as a result from long-time continuous deposition and uptake of materials from the ground (Schutz and Sebert, 1987). The cluster analysis is conducted using the statistical software SPSS Statistics 17.0 (SPSS Inc.). As hierarchical cluster analysis is applied to each site, more than 600 daily data covering 2000-2007 period are involved for ~90% of 68 sites except for a few sites with missing data. In the cluster analysis, the concentrations of Si, Ca, K, Fe, Ti, As, Cu, Pb, S, Zn and V, $PM_{2.5}/PM_{10}$ ratio, and the enrichment factors of Ca, K, Fe, As, Cu, Pb and Zn, are used to construct six clusters. The concentrations of five aerosol components, Al, sulfate, nitrate, OC and EC are excluded from this analysis to avoid the unbalanced sampling issue, because a large portion of these data are either missing or invalid. Between-Group Linkage clustering method and Pearson Correlation to measure inter-cluster intervals are configured to assemble the most similar cases into a same group. This method measures the correlations of x and y variables of case i according to the following formula (SPSS Statistics 17.0 Algorithms, SPSS Inc.):

$$C_{xy} = \frac{\sum_i (Z_{xi} Z_{yi})}{N} \tag{2}$$

$$Z_{xi} = \frac{Xi - \overline{X_N}}{\sqrt{\sum (Xi^2 - \overline{X_N}^2)/(N-1)}} \tag{3}$$

Where C_{xy} the correlation between variable x and variable y, Z_{xi} and Z_{yi} are the standardized Z-score value of x and y for the case i, respectively, N is the number of cases, and $\overline{X_N}$ is the average value of x of the case i (x_i) for the N cases. The cases with higher correlation, which means higher similarity, are put into one cluster (or group).

In this study, the cluster analysis processes daily aerosol data (i.e., 24-hour every third day according to the IMPROVE sampling protocol) at each site to identify a dust group. During the study period, there are more than 600 daily data records from 90% of studied 68 sites except for a few sites with less than 300 data records. After the cluster analysis, the identified dust records at each site are further grouped according to the geographic locations and temporal ranges for subsequent analysis.

2.2 Observational data

The aerosol observation data from the IMPROVE network were chosen for two reasons. The IMPROVE monitoring sites, with a few exceptions, are deployed in the national parks and wilderness areas in the United State (Pitchford and Malm, 1994), including many sites in close proximity or downwind to major dust source regions. Second, the IMPROVE network is also one of the two national air quality monitoring networks that measure both mass concentrations and chemical composition of atmospheric aerosols. There are other national or regional monitoring networks existing in the United States. The EPA Air Quality System (AQS) network has a national coverage, but there is no aerosol composition data available from this network. Another national aerosol monitoring network, the Chemical Speciation Network (CSN), is deployed mostly in urban areas, making it unsuitable for dust monitoring due to anthropogenic contamination. There are also some regional networks, such as the Southeastern Aerosol Research and Characterization Study (SEARCH), which measures aerosol mass and composition at both urban and rural sites (Edgerton et al., 2009). The currently operating eight SEARCH sites, however, are located in the southeastern US and are too far away from major dust sources.

A subset of 68 sites from the IMPROVE network are used in this study. This subset of IMPROVE sites, deployed in eight western states (Fig. 1), is chosen based on the findings in previous studies that have identified the geographical distribution of active dust sources in the North America (Gillette and Passi, 1988; Malm et al., 2004; Van Curen, et al., 2002; Wells et al., 2007; Draxler et al., 2010). These regions are generally associated high wind power over barren land. The IMPROVE samplers have four modules designed to collect samples to measure PM_{10} and $PM_{2.5}$ mass concentrations, and $PM_{2.5}$ chemical components (Malm et al., 1994). These aerosol components include 24 elements (Al, As, Br, Ca, Cl, Cr, Cu, Fe, K, Mn, Mo, Na, Ni, P, Pb, Rb, S, Se, Si, Sr, Ti, V, Zn, Zr) measured by proton-induced X-ray emission (PIXE) and X-ray fluorescence (XRF), selected ions (Cl^-, NO_3^-, $SO_4^=$) by ion chromatography (IC), organic to elemental carbon ratio (OC/ EC) by staged thermal desorption and combustion, and total hydrogen by proton elastic scattering (PESA) (Malm, 2000). Fine soil in the IMPROVE data is calculated from the mass concentrations of five major soil-derived elements (Al, Si, Ca, Fe, K, and Ti) in their assumed oxides (Al_2O_3, SiO_2, CaO, K_2O, FeO, Fe_2O_3, TiO_2, respectively) (Malm, 2000a, 2000b):

$$Soil_f = 2.2[Al] + 2.49\,[Si] + 1.63[Ca] + 2.42[Fe] + 1.94[Ti] \quad (3)$$

where [Al], [Si], [Ca], [Fe] and [Ti] are the measured concentrations of particulate Aluminum, Silicon, Calcium, Iron and Titanium, respectively. All observational data for the period 2000-2007 are used in the subsequent analyses. All data flagged in the dataset for not attaining quality control standards were removed, with the exception of those flagged for moderate changes in flow rate. Data from the IMPROVE sites east of Kansas are excluded from this analysis, since there are no major active dust sources in this region.

Besides the IMPROVE data, satellite remote sensing of dust aerosols is used to independently identify local dust events. The MODIS sensors aboard both Terra and Aqua have been making global daily observations of atmospheric aerosols since 2002 (Terra started in 2000). A total of seven wavelength channels (ranging from 0.47 to 2.13 μm) are used by MODIS to retrieve aerosol properties. Separate algorithms are developed for aerosol retrieval over land and ocean. Over the ocean, MODIS relies on the aerosol spectral signature from 0.55 to 2.13 μm to separate pollution particles (smaller in size) from coarse sea-salt and dust particles (Tanré et al., 1997). Over the land, MODIS uses the 2.1 mm channel to monitor surface-cover properties, and the visible wavelength to observe surface reflectance (Kaufman et al., 1997).

3. Identifying windblown dust events

3.1 Analysis of satellite detected dust events

During the study period, there were thirteen large dust storms occurring in the southwestern United States that have been identified from NASA Earth Observatory's Natural Hazards dust products (http://earthobservatory.nasa.gov/NaturalHazards). The purpose of analyzing these known dust events is to learn from these data of the distinct physical and chemical properties of local dust samples. The IMPROVE sampling protocol is to collect a 24h duration sample every three days. Therefore, it is difficult for the ground monitors to capture all dust events identified by the satellite sensors. Meanwhile, because of limited temporal and spatial coverage, cloud contamination and high surface reflectivity over deserts, satellite remote sensing can not detect all dust events. Therefore, it is not easy to pinpoint a dust case that is simultaneously recorded by both satellite sensors and ground monitors. Here we focus on three such rare dust cases that were recorded by both ground and satellite observations on April 15, 2003, November 27, 2005 and April 12, 2007. The MODIS imageries show that the three storms originated from different source regions. The former two storms were conceived from the Chihuahuan Desert in northern

Mexico, while the latter one from the Mojave Desert in southern California. By examining the MODIS imageries and the PM_{10} concentrations at ground monitors, we choose one or two IMPROVE sites that have captured a significant amount of dust aerosols at their samplers. These sites include the Guadalupe Mountains National Park, TX (GUMO1) site for the April 15, 2003 storm, the Big Bend National Park, TX (BIBE1) site and the GUMO1 site for the November 27, 2005 storm, and the Agua Tibia, CA (AGTI1) site and the San Gorgonio Wilderness, CA (SAGO1) site for the April 12, 2007 storm (Fig. 2).

The aerosol mass and chemical composition measurements at these monitors are then used to extract the commonality of typical local dust samples. In each case, we compare the observed concentrations of PM_{10}, $PM_{2.5}$, crustal (Si, Ca, Fe, K) and anthropogenic elements (Cu, Zn, Pb), sulfate, nitrate, OC and EC in $PM_{2.5}$, the $PM_{2.5}/PM_{10}$ ratio, the percentage of the above species and the enrichment factors of anthropogenic elements before, during, and after these dust episodes (Fig 2). A few interesting patterns are shown in the aerosol samples collected during dusty periods: 1) compared to that on non-dusty days, the PM_{10} concentration during a dusty day was elevated by 2–10 times from the pre-storm and post-storm levels; 2) although the concentration of $PM_{2.5}$ also increased during a dust storm, the $PM_{2.5}/PM_{10}$ ratio dropped significantly to approximately 0.2, a value typically representing freshly emitted soil particles; 3) both the concentrations and percentage of crustal elements, including Si, Ca, Fe, and K, increased during dusty days; 4) The percentages of anthropogenic components in $PM_{2.5}$, including Cu, Zn, Pb, SO_4^{2-}, NO_3^-, and OC, all decreased from their corresponding pre-storm and post-storm levels, although the absolute concentrations may have increased or decreased depending on the site and the species. The concentration of EC during the dusty days was reduced to almost zero at all sites, but sulfate and nitrate concentrations varied at different sites, with an increase at the GUMO1 site and the BIBE1 site during the November 2005 dust storms and a decrease at the AGTI1site and the SAGO1 site during the April 2007 dust storm. The concentrations of particulate sulfate and nitrate during dust events are controlled by two processes: the dilution by dusty but otherwise clean air of background pollution (Guo et al., 2004) and the supply of sulfate and nitrate from soil particles and the uptake and/or formation of nitrate and sulfate on dust particles. Similar phenomena have been reported in previous studies (Arimoto et al., 2006; Wang et al., 2005, Sun et al., 2004) in which the concentrations of nitrate and sulfate increased during dust days, since mineral dust particles provide alkalic surface and

catalytic for the scavenging and heterogeneous conversion of SO_2 and NO_x into sulfate and nitrate. For the selected cases, the absolute concentrations of sulfate and nitrate increase, but the relative abundance of these components decreases (Fig 2); and 5) The silicon enrichment factors of Cu, Zn and Pb, which indicates anthropogenic contamination, decreased dramatically on dusty days.

Although the number of dust storms analyzed here is limited, the consistence of these patterns at all sites suggests that it may be feasible to identify local dust events through the use of routinely monitored aerosol parameters. Based on the observations above, we propose the following five indicators to be used to identify local dust records in the subsequent hierarchical cluster analysis: 1) high PM_{10} concentrations; 2) low ratio of $PM_{2.5}$ to PM_{10}; 3) higher concentrations and percentage of crustal elements; 4) lower percentage of anthropogenic pollutants; and 5) low enrichment factors of anthropogenic elements.

3.2 Cluster analysis

After establishing these identifying indicators, we use cluster analysis to test the hypothesis that there is one aerosol group, the local dust group, simultaneously matching all the above selection criteria. We perform hierarchical cluster analysis for all validated aerosol measurement data over the 68 study sites, using the concentrations of PM_{10}, $PM_{2.5}$, elements (Si, Ca, K, Fe, Ti, As, Cu, Zn, Pb, V), the $PM_{2.5}$ to PM_{10} ratio, the enrichment factors of K, Ca, Cu, Zn and Pb as the clustering criteria as discussed earlier. We found that over 30 of the 68 sites, there is one aerosol data group that demonstrates similar physical and chemical characteristics as observed in the previously satellite identified dust events. At the remaining sites, none of the IMPROVE data show any consistent pattern of dust events.

Figures 3 and 4 show the results of cluster analysis of all IMPROVE observation data from 2000 to 2007 at the GUMO1 site, which experienced the large number of dust storms during the study period. The cluster analysis divides all data into six groups, and the first group has the highest PM_{10} concentrations (Fig. 3a). The mean PM_{10} concentration in this group is approximately 60 $\mu g/m^3$, 3–10 fold of the typical background levels in the western United States (Malm et al., 1994). The $PM_{2.5}$ concentrations in this group are also higher than in other groups, although the differences among groups are relatively smaller than that for the PM_{10} concentrations (Fig. 3b). The concentrations of the four crustal elements are significantly higher

in group 1 than in other groups (Fig. 3c). During non-dusty days, the concentrations of these crustal elements in $PM_{2.5}$ are low (less than 0.1 μg/m^3) in most cases, except for Si the concentration of which reaches 1.0 μg/m^3 occasionally. During dust storms, the Si concentration varies from 1.0 μg/m^3 to 6.0 μg/m^3. For the three trace metals that are mainly attributed to anthropogenic sources, their concentrations in group one is among the lowest, but the difference is not as distinguishable as that of PM_{10} or crustal elements (Fig. 3e), likely resulting from varying meteorological conditions and uneven distribution of emission sources. For the four major aerosol components (sulfate, nitrate, OC and EC), the distinction among these groups is further blurred. This is because these aerosol components can be contributed by both natural soil dust and non-dust sources (Fig. 3e). Finally, the data in group one have the lowest $PM_{2.5}/PM_{10}$ ratios. The $PM_{2.5}/PM_{10}$ ratio ranges from 0.1 to slightly above 0.3, with a mean of 0.2. The ratios in other groups have a wide range, from 0.1 to over 0.9 (Fig. 3f). The higher ratio reflects either higher contribution of anthropogenic sources and biomass burning, or the aging of aerosol plumes.

Figure 4 shows additional distinct physical and chemical characteristics of group 1 from other data groups. Not only the actual mass concentrations of crustal elements are higher in group 1, their relative abundance (in percentage) is also higher than in other groups (Fig 4a). The opposite is true for the three anthropogenic trace metals, the percentage of which is the lowest among all groups. The enrichment factors for these metal elements are extremely close to unity in group 1, indicating their soil origin. In comparison, the silicon referenced enrichment factors are much higher in all other groups, except group 4, which shows consistent low enrichment factors and higher crustal elements. This group, although not as clearly characterized as group 1, may represent similar soil dominated aerosol samples, such as smaller dust events or anthropogenic soil dust (such as from unpaved road or mining operation). Based on the consistent and distinct chemical and physical patterns that simultaneously match the five stipulated criteria, we hence identify group 1 from the cluster analysis as the local dust aerosol group.

Figure 5 shows all identified dust events along the time series of $PM_{2.5}$ and PM_{10} concentrations at the GUMO1 site during the entire study period. Most of the high PM_{10} cases are identified by the cluster analysis as local dust events (highlighted with dashed circles), including the two large dust storms discussed in section 3.1. However, there are other cases of high PM_{10} concentrations being excluded by the cluster analysis as local dust samples. These

data are either associated with high $PM_{2.5}$ to PM_{10} ratios (long-distance dust transport or biomass burning) or with different chemical composition (i.e., aerosols originated from other sources).

4. Summary of identified dust records

4.1 Summary of identified dust records

Cluster analysis of all aerosol data identifies a total of 182 dust records from 30 of the 68 sites (Table 1). These sites with dust records are also marked in red in Figure 1. These 30 sites are located in the states of Texas, New Mexico, Arizona, South California, Nevada and Colorado. Such spatial distribution is consistent with the distribution of the four U.S. Deserts, namely the Great Basin Desert, the Mojave Desert, the Sonoran Desert, and the Chihuahuan Desert. Outside the deserts, there are two sites in Colorado where previous model studies have found that high wind power in spring lifts surface soil grains (Gillette and Hansen, 1989). Overall, the spatial distribution is similar to the dust source map reported in previous studies (Malm et al., 2004; Kavouras et al, 2007).

Among the 30 dust sites, there are three sites, including Phoenix (PHOE1) and Douglas (DOUG1) in Arizona, and Fresno (FRES1) in California, that demonstrate distinct patterns in chemical composition. Although all located in arid or semiarid regions, these sites are also noticeably influenced by anthropogenic sources from nearby urban areas. In fact, a separate cluster has been identified for these sites, where the concentrations and percentage of primary anthropogenic pollutants such as Cu, Zn, Pb and EC, as well as their enrichment factors are much higher than at rural or remote dust source areas. The concurrent high crustal and anthropogenic elements result from strong mixing of wind-generated emissions and urban plumes, a unique setting for studying the interactions between dust and urban pollutants.

4.2 Temporal and spatial variability in dust events

The temporal variability of dust aerosols is also an interesting feature to air quality and climate modeling. Previous windblown dust studies, mostly relying on model simulations, predicted a springtime maximum over the North America (Gillette and Hansen, 1989; Tegen and Miller, 1998). The “well-known” seasonal trend of local windblown dust in US, however, has not been independently evaluated against robust measurement data except for Kavouras et al.

(2007), who used wind and visibility data to identify local windblown dust and investigated the seasonal trend.

The dust events identified in this work display large temporal and spatial variability. All dust cases from the three urban sites are excluded here because of their proximity to urban emissions. Figure 6 shows the interannual variations of local dust records in the five dust regions from 2000 to 2007. Although the IMPROVE monitors are not expected to capture all dust events, the dust records over these static sites nevertheless reflect the year-to-year change in dust activities over these areas. Unlike urban monitors, the IMPROVE monitors are distributed far away from each other. Therefore, the observed dust events are unlikely to overlap those detected at other locations. Only during extraordinarily large dust events, such as the April 15, 2003 storm, the dust plume can be detected by multiple IMPROVE monitors (four in this case) and the data at these sites are considered valid since all five filtering criteria are met.

During the eight-year study period, the total number of dust events displays an interesting four-year activity cycle. In the first cycle, the dust events increase from 8 per year in 2000 to 45 per year in 2003. In the second cycle, dust activities dropped to below 10 per year in 2004, and then persistently increase to 20 per year in 2007. It is not clear if such an interannual pattern exists in other years. The years of 2003, 2002 and 2007 are the three most active dust periods, with 46, 31 and 24 recorded dust events, respectively. The years of 2000, 2004 and 2005 are the calmest dust periods, all with single digit dust records.

Figure 6 also reveals the different activity patterns in different dust regions. The Chihuahuan Desert (59 cases) and the Sonoran Desert (62 cases) are by far the most active source regions. In general, the Chihuahuan Desert dominates dust activities in the first half while the Sonoran Desert in the second one (Fig. 6). The interannual trend is primarily driven by the dust activities from these regions. The Mojave Desert contributes 23 dust events during this period, while the Great Basin Desert and the Colorado Plateau contribute only seven and eight dust events, respectively.

The dust records suggest clear seasonal variability in dust activities. The monthly frequency of dust events (Fig. 7) shows a peak from March to July and a second peak in autumn from September to November. Among all months, the highest number of dust records is in April, when the dust emissions in both the Chihuahuan and Sonoran Deserts are most active. The month of May sees almost the same number of dust events as April, because the increase of dust

activities in the Sonoran Desert can largely offset the diminished activities in the Chihuahuan Desert. Actually, May 2003 is the month with the largest number of local dust records during the eight-year period, with 16 dust records obtained by 10 IMPROVE monitors there. The abundance of ground measurements during this period makes it an ideal case for a future dust modeling study over the United States. The peak dust season in the Chihuahuan Desert is about two months earlier than in Sonoran Desert. The lowest number of dust events is found in January and August, during both periods dust activities were found only in the Mojave Desert. During the study period, there are eight sites that have observed more than eight local windblown dust events, with the GUMO1 site in Texas having the largest number (27) of dust records. In addition, the Queen Valley site in Arizona (QUVA1), the Big Bend site in Texas (BIBE1), the Salt Creek site in New Mexico (SACR1), the Chiricahua site (CHIR1), the Saguaro West site (SAWE1), and the Ike's Backbone site (IKBA1), all in Arizona, have captured 19, 16, 12, 9, 9, and 9 dust events, respectively. These monitors are either located in or downwind to the previously identified dust source regions associated with the geological characteristics of high soil erodibility (Kavouras et al., 2007).

5. Discussion

5.1 Limitations with the dust identification approach

The major limitation of our approach is that the dust indictor parameters may not be universally available from routine aerosol monitoring networks. Our approach involves both physical and chemical data of aerosol measurements, therefore requiring a comprehensive monitoring and analysis networks such as the IMPROVE program used in this study. In many cases, especially over major dust active regions over Africa and Asia, routine measurements of aerosol size distribution and chemical composition are not available. The lack of these aerosol parameters limits the applicability of our approach to dust studies for those regions.

Alternatively, we consider here three simplified methods that use only basic aerosol mass concentrations, and compare their capability to pinpoint dust events to that of the full method using all five indicators. The first simplified approach uses two dust indicators, the PM_{10} mass concentration (> 40 $\mu g/m^3$) and the $PM_{2.5}/PM_{10}$ ratio (< 0.35) as the filtering criteria. The PM_{10} cutoff and the $PM_{2.5}/PM_{10}$ ratio cutoff are taken from the lower and upper 95% values of the corresponding parameters in the local dust group identified by the full method as proposed in this

study, respectively. The second method is similar to the first one, except using a $PM_{2.5}/PM_{10}$ cutoff of 0.20, the median value of the dust group. This ratio is also used by the US EPA to split fugitive dust PM_{10} into $PM_{2.5}$ (MRI, 2005). Compared to the first one, the second method is considerably more exclusive. The third method simply uses $PM_{10} > 100$ μg/m^3 as the identifying indictor, following Ganor et al. (2009). Due to the IMPROVE sampling protocols, 24-hour mean PM_{10} concentrations are used here, instead of hourly PM_{10} data as in Ganor et al. (2009). Table 2 compares the performance of the three simplified methods to identify dust events to that of the full method. Here we define the performance using two categorical evaluation metrics as introduced by Kang et al. (2009): Hit Rate and False Alarm Ratio. Hit Rate is the percentage of "true" dust events identified by the simple method to all events by the full method, while the False Alarm Ratio is the percentage of "false" events (i.e., not considered local dust events by the full method) to all events selected by the simple methods. The first simplified method has the highest hit rates, catching 27% of the dust events identified by the full method. Meanwhile, it is also associated with the highest false alarm ratio, with 68% of the dust events it selected deemed false by the full method. When the $PM_{2.5}/PM_{10}$ ratio is further constrained to 0.20, the false alarm ratio has been reduced significantly (to 16%), but at the cost of hit rate, which shows that the second method can catch only 13% of the all dust events. The revised Ganor method demonstrates dust identifying capability between the two simplified methods. Although these simplified methods show varying effectiveness to identify local dust events, it should be pointed out that chemical fingerprint is still needed to assure the origin of measured aerosols. For example, the measurement data over the three urban sites can satisfy all selection criteria for local dust events, except the high levels of anthropogenic components. Such information reveals either human contamination of the dust aerosols, or human motivated dust sources (such as road dust from unpaved road). Regardless of its complexity, our proposed approach is likely to work most efficiently when all five identification criteria are concurrently applied.

5.2 Dust activities in the western United States

Our study reveals that dust events in the United States occur in almost all seasons, suggesting the prevailing impact of windblown dust across the year. This seasonal variation is consistent with previous model simulation over the United States (Gillette and Hansen, 1989; Park et al., 2010). The windblown dust emissions peak in the spring, due to high wind speed, low soil moisture, and a lack of vegetation cover over erodible land surface. The springtime maximum

over North America was also reported in a long-term general circulation model study by Tegen and Miller (1998). Some previous study (e.g. Gatz and Prospero, 1996) has used the infrequency of summertime dust plumes to exclude the possibility of the impact of dust storms on regional air quality. This work and several previous modeling studies suggest that it is possible to see summertime impact of dust aerosols originated from the western United States.

Although the IMPROVE sites are not expected to capture all dust events on a local scale, in particular for the Great Basin Desert and southern Chihuahuan Desert where monitors are sparse, a dataset of observed dust events developed from using our approach can help evaluate the completeness or efficiency of satellite-based approaches. Meanwhile, a variety of computer models have been developed to study the life cycle of dust aerosols and their effects on the regional and global climate systems. Although dust sources over North America contributes to only 3% of global dust budget (Ginoux et al., 2001), previous model simulations have highlighted the importance of dust aerosols in regional air quality and climate modeling over the western United States (Draxler et al., 2010). The same observed dust dataset can provide detailed comparisons between model and observations on an event level. Furthermore, the rich pool of aerosol chemical composition data associated with these identified dust records are useful to compile chemical profiles for splitting dust aerosols. Recent advances of aerosol modeling (such as the latest version of the Community Multiscale Air Quality (CMAQ) model) require emission information of not only the mass flux and size distribution, but also the chemical composition of emitted dust particles. A companying paper (Dan et al., Chemical composition of natural dust particles in the United States, in preparation) utilizes the data of the identified dust events and chemical composition to derive chemical profiles that could be used in future dust aerosol emission and modeling works.

Dust activities display a four-year cycle during the eight-year study period. While more data are needed to verify this four-year cycle observed in this study, we discuss briefly here the possible driving forces behind this interannual variability. Climate models have predicted that a transition to a more arid climate is under way in the southwestern United States, where multiyear drought and the 1930s Dust Bowl will become the new climatology within a time frame of years to decades (Seager et al., 2007). Windblown dust emissions are controlled by a number of important parameters, such as wind speed, soil moisture, surface roughness and erodible dust supply (Marticorena et al., 1995; Gillette et al., 1988; 2004). Among these controlling factors,

surface wetness can be used as an indicator to drought condition, which is often associated with dust activities in arid environment. Here we examine the monthly surface wetness over the five dust regions using the Modern Era Retrospective-analysis for Research and Application (MERRA) dataset from the NASA's Goddard Space Flight Center (http://gmao.gsfc.nasa.gov/research/merra/). Figure 8 shows that the lowest surface wetness is found in different months among these regions. The Chihuahuan Desert generally sees an early dry season, while the Sonoran Desert and the Mojave Desert are often associated with a prolonged and drier summer. Although soil moisture controls several factors that influence dust emissions, the monthly surface wetness data here are not in good correlation with the observed dust pattern. The monthly regional mean of surface wetness may not represent the local condition under which dust emissions are initiated. As discussed by many field and model studies, windblown dust emission is a complicated process that has not been fully understood. In addition, these processes are increasingly complicated by human disturbance of the land surface, such as the rapid urbanization in southern Arizona (Sorooshian et al., 2011). Future analysis of the meteorological parameters and surface conditions over these regions is need to further investigate the underlying mechanisms causing the interannual variations. Given the climate model prediction of a drier climate in the Southwest, it is interesting to continue observing how the dust activities will respond to the changes in regional and global climate systems.

6. Conclusions

Dust is a major component of atmospheric aerosols in many parts of the world. There are, however, very few monitoring networks that are exclusively designed and deployed to observe sand and dust particles. General-purpose aerosols monitoring networks, however, exist in a large number. The approach we propose here can utilize the general aerosol observations to identify local dust events. Using the publicly available IMPROVE aerosols, we demonstrate how to use an observation-based approach to pinpoint 182 local dust records over 30 locations in the western United States over a eight-year study period.

The results presented in this study are subject to several limitations. The IMPROVE monitors are unevenly deployed over different dust source regions. Therefore, the observation-based dust data may not represent the overall emissions from each region. For instance, there are only five monitors in the Great Basin Desert, and none is sitting in the heart of the barren land.

The low number of recorded dust events (about one in each year) may be related to the sparse monitors in this region. Meanwhile, the IMPROVE monitors are more densely deployed over the Sonoran Desert and north Chihuahuan Desert. The high number of dust records over these regions reflects both dense detection and active dust emissions.

Although our method specifically targets local dust samples, it can be easily extended to pinpoint other intermittent emission sources, such as long-range transported dust, volcanic ash, and biomass burning. Long-range transported dust is also associated with an increase in crustal elements. Compared to local dust events, the increase in mass concentration from the non-dusty level may be smaller, and the $PM_{2.5}/PM_{10}$ ratio is much higher during a long-range transport event (Cheng et al., 2005). The volcanic ash or dry fog formed from emitted sulfate dioxide is associated with high levels of sulfate content in the aerosols (Bao et al., 2010). The high sulfate and low anthropogenic elements can be used to distinguish these data from that featuring coal-burning aerosol. Similarly, biomass burning originated aerosols contain high levels of potassium, organic carbon and black carbon, and the aerosols are predominantly in the fine mode (Reid et al., 2005). Through a reasonable procedure of remote sensing-assisted data training, our method can be applied to identify a number of distinct aerosol sources in research and regulatory applications. Our approach emphasizes using ground monitoring data for dust identification. In this approach, the use of satellite data is limited to selecting independently identified dust events for the purpose of methodological training. There are other approaches that rely predominantly on remote sensing data to pin-point dust events (Prospero et al, 2002; Lee et al, 2009; Rivera-Rivera et al., 2010). Our study proposes an alternative way to pin-point dust events that can work complimentarily with these satellite-based methods to identify dust events.

Acknowledgement:
This work is financially supported by NOAA Air Resources Laboratory (DQT and MD) and by the Beijing Municipal Institute of Labor Protection (MD and TW). The authors thank ARL Director Dr. Steve Fine for initiating this project, and our late colleague Dr. Daewon Byun for inspiring discussions. The constructive comments from two ARL internal reviewers and three anonymous external reviewers are also gratefully acknowledged.

References

Arimoto, R., Kim,Y.J., Kim, Y.P., et al., 2006. Characterization of Asian Dust during ACE-Asia. Global and Planetary Change 52, 23–56.

Bao, H.M., S. Yu, and Tong, D.Q., Massive volcanic SO_2 oxidation and sulphate aerosol deposition in Cenozoic North America, *Nature*, 465: 909-912, 17 June 2010.

Bell, M. L., F. Dominici, K. Ebisu, S. L. Zeger, and J. M. Samet, 2007. Spatial and Temporal Variation in PM2.5 Chemical Composition in the United States for Health Effects Studies. *Environmental Health Perspectives*, 115(7), 989-995.

Cheng, T., D. Lu, G. Wang, Y. Xu, 2005. Chemical characteristics of Asian dust aerosol from Hunshan Dake Sandland in Northern China. Atmospheric Environment, 39 (2005), pp. 2903–2911.

Chow, J.C., J.G. Watson, D.H. Lowenthal, P.A. Solomon, K.L. Magliano, S.D. Ziman, L.W. Richards, 1993. PM_{10} and $PM_{2.5}$ compositions in California's San Joaquin Valley. Aerosol Sci. Technol., 18 (1993), pp. 105–128.

Chow, J. C.; Watson, J. G.; Ashbaugh, L. L.; Magliano, K. L., 2003. Similarities and differences in PM10 chemical source profiles for geological dust from the San Joaquin Valley, California. *Atmos. Environ. 37*, 1317.

Dorling, S.T., David, T.D., Pierce, C.E., 1992. Cluster analysis: a technique for estimating the synoptic meteorological controls on air and precipitation chemistry—method and applications. Atmospheric Environment 26A, 2575–2581.

Draxler, R. R., P. Ginoux, and A. F. Stein (2010), An empirically derived emission algorithm for wind-blown dust, *J. Geophys. Res*., 115, D16212, doi:10.1029/2009JD013167.

Edgerton, E.S, G.S. Casuccio, R.D. Saylor, T.L. Lersch, B.E. Hartsell, J.J. Jansen and D.A. Hansen, 2009. Measurements of OC and EC in coarse particulate matter in the southeastern United States. *J Air Waste Manag Assoc.* 2009 Jan;59(1):78-90.

Escudero, M., Querol, X., Pey, J., Alastuey, A., Pe´ rez, N., Ferreira, F., Alonso, S.,Rodrıguez, S., Cuevas, E., 2007. A methodology for the quantification of the net African dust load in air quality monitoring networks. Atmospheric Environment 41, 5516–5524.

Fairlie, T.D., D.J. Jacob, and R.J. Park, 2007. The impact of transpacific transport of mineral dust in the United States, *Atmospheric Environment*, 41, pp 1251-1266.

Ganor, E., A. Stupp, P. Alpert, 2009. A method to determine the effect of mineral dust aerosols on air quality. Atmospheric Environment, 43, 5463-5468.

Gao Y., J.R. Anderson, X. Hua, 2009. Dust characteristics over the North Pacific observed through shipboard measurements during the ACE-Asia experiment. Atmospheric Environment 41 (2007) 7907–7922.

Gatz, D.F., and J.M. Prospero, A large silicon-aluminum aerosol plume in central Illinois: North African desert dust? *Atmos. Environ*., 30, 3789-3799, 1996.

Gillette, D.A., and R. Passi (1988), Modeling dust emission caused by wind erosion. *J. Geophys. Res.*, 93, 14,233-14,242.

Gillette, D.A., and K. Hanson (1989), Spatial and Temporal Variability of Dust Production Caused by Wind Erosion in the United States, J. Geophys. Res., 94(D2), 2197-2206.

Gillette, D.A. and A. Pitchford, 2004: Sand flux in the northern Chihuahuan Desert, New Mexico, USA, and the influence of mesquite-dominated landscapes. *J. Geophys. Res.*, 109, 1-12. F04003, doi:10.1029/2003JF000031.

Ginoux, P., M. Chin, I. Tegen, J. M. Prospero, B. Holben, O. Dubovik, and S. Lin (2001), Sources and distributions of dust aerosols simulated with the GOCART model, *J. Geophys. Res.*, *106*(D17), 20,255–20,274.

Gong, S. L., X. Y. Zhang, T. L. Zhao, I. G. McKendry, D. A. Jaffe, and N. M. Lu (2003), Characterization of soil dust aerosol in China and its transport and distribution during 2001 ACE-Asia: 2. Model simulation and validation, *J. Geophys. Res.*, *108*(D9), 4262, doi:10.1029/2002JD002633.

Guo, J, Rahn, K. A., Zhuang, G., 2004. A mechanism for the increase of pollution elements in dust storms in Beijing. Atmospheric Environment, 38, 855–862.

Hu, X. Q., Lu, N. M., Niu, T., and Zhang, P.: Operational Retrieval of Asian Dust Storm from FY-2C Geostationary Meteorological Satellite and its Application to real time Forecast in Asia, Atmos. Chem. Phys., 8, 1649–1659, 2008, http://www.atmos-chem-phys.net/8/1649/2008/.

Intergovernmental Panel on Climate Change (IPCC), 2007. Climate Change 2007: The Physical Science Basis, Summary for Policymakers, IPCC Secretariat, World Meteorol. Organ.,, Geneva, Switzerland.

Jaffe, D., Bertschi, L. Jaegle, P. Novelli, J. S. Reid, H. Tanimoto, R. Vingarzan, and D. L. Westphal (2004), Long-range transport of Siberian biomass burning emissions and impact on surface ozone in western North America, Geophys. Res. Lett., 31, L16106, doi:10.1029/2004GL020093.

Kang, D., R. Mathur, K. Schere, S. Yu and B. Eder, 2007: New Categorical Metrics for Air Quality Model Evaluation, Journal of Applied Meteorology and Climatology, 46:549-555.

Kaufman, Y. J., D. Tanre´, L. A. Remer, E. F. Vermote, A. Chu, and B. N. Holben, Operational remote sensing of tropospheric aerosol over land from EOS moderate-resolution imaging spectroradiometer, J. Geophys. Res., 102, 17,051– 17,067, 1997.

Kavouras, I. G., V. Etyemezian, J. Xu, D. W. DuBois, M. Green, and M. Pitchford (2007), Assessment of the local windblown component of dust in the western United States, *J. Geophys. Res.*, 112, D08211, doi:10.1029/2006JD007832.

Kim, K., et al., 2003: The chemical composition of fine and coarse particles in relation with the Asian dust events. *Atmos. Environ.*, **37**, 753-765.

Lee, J.A., T.E. Gil, K.R. Mulligan, M. Dominguez Acosta, A.E. Perez (2009). Land use/land cover and point sources of the 15 December 2003 dust storm in southwestern North America. Geomorphology 105: 18-27.

Luo, C., N. M. Mahowald, and J. D. Corral, 2003: Sensitivity study of meteorological parameters on mineral aerosol mobilization, transport, and distribution, *J. Geophys. Res.*, 108(D15), ???, doi:10.1029/2003JD003483.

Malm, W. C., J. F. Sisler, D. Huffman, R. A. Eldred, and T. A. Cahill (1994), Spatial and seasonal trends in particle concentration and optical extinction in the United States, *J. Geophys. Res.*, 99(D1), 1347–1370, doi:10.1029/93JD02916.

Malm, W., 2000a. Spatial and seasonal patterns and temporal variability of haze and its constituents in the United States Report III. Cooperative Institute for Research in the Atmosphere, Colorado State University, Fort Collins, CO 80523, ISSN: 0737-5352-47.

Malm, W. C., et al. (2000b), IMPROVE (Interagency Monitoring of Protected Visual Environments): Spatial and seasonal patterns and temporal variability of haze and its constituents in the United States: Report II, CIRA Report ISSNL 073705352-47, Colo. State Univ. Fort Collins.

Malm, W.C., Schichtel, B.A., Pitchford, M.L., Ashbaugh, L.L., Eldred, R.A., 2004. Spatial and monthly trends in speciated fine particle concentration in the United States. *J. Geophys. Res.*, 109, D03306, doi:10.1029/2003JD003739.

Marticorena, B., G. Bergametti, (1995). Modeling the atmospheric dust cycle: 1. Design of a soil-derived dust emission scheme. Journal of Geophysical Research. V.100 (#D8). Pg. 16,415-16,430.

Midwest Research Institute (MRI), 2005. Analysis of the Fine Fraction of Particulate Matter in Fugitive Dust. MRI Project No. 110397. Available online at: http://www.epa.gov/ttnchie1/ap42/ch13/related/mri_final_fine_fraction_dust_report.pdf (last accessed on May 10, 2012).

Nicolas, J., M. Chiari, J. Crespo, I. DG. Orellanan, F. Lucarelli, S. Nava 2008. Quantification of Saharan and local dust impact in an arid Mediterranean area by the positive matrix factorization (PMF) technique. Atmospheric Environment. 42, 8872-8882.

Park, S. H., S. L. Gong, W. Gong, P. A. Makar, M. D. Moran, J. Zhang, and C. A. Stroud (2010), Relative impact of windblown dust versus anthropogenic fugitive dust in $PM_{2.5}$ on air quality in North America, *J. Geophys. Res.*, 115, D16210, doi:10.1029/2009JD013144.

Pitchford, M.L., W.C. Malm, 1994. Development and applications of a standard visual index. Atmospheric Environment. 28(5), p1049-1054.

Prospero, J.M., and T.N. Carlson, Radon-222 in the North Atlantic trade winds: Its relationship to dust transport from Africa, Science, 167, 974-977, 1970.

Prospero, J.M., Long-term measurements of the transport of African mineral dust to the southeastern United States: Implications for regional air quality, *J. Geophys. Res. ,104*(D13), 15,917-15,927, 1999.

Prospero, J.M., P. Ginoux, O. Torres, S.E. Nicholson,and T.E. Gill, 2002. Environmental characterization of global sources of atmospheric soil dust identified with the NIUBUS 7 Total Ozone Mapping Spectrometer (TOMS) absorbing aerosol product. Reviews of Geophysics, 40 (1) 2-1. doi:10.1029/2000RG000095.

Reff, A., Bhave, P.V., Simon, H., Pace, T.G., Pouliot, G.A., Mobley, J.D., Houyoux, M., 2009, Emissions inventory of $PM_{2.5}$ trace elements across the United States, *Environmental Science and Technology*, 43, 5790-5796.

Reid, J. S., et al., Analysis of measurements of Saharan dust by airborne and ground-based remote sensing methods during the Puerto Rico Dust Experiment (PRIDE), J. Geophys. Res., 108(D19), 8586, doi:10.1029/2002JD002493, 2003.

Reid, J.S., R. Koppmann, T.F. Eck, and D.P. Eleuterio, A review of biomass burning emissions part II: intensive physical properties of biomass burning particles. Atmos. Chem. Phys., 5, 799–825, 2005.

Rivera-Rivera N.I., T.E. Gill, M.P. Bleiweiss, J.L. Hand (2010). Source characteristics of hazardous Chihuahuan Desert dust outbreaks. Atmospheric Envrironment 44(20): 2457–2468.

Schepanski, K. I. Tegen, B. Laurent, B. Heinold, and A. Macke, 2007, A new Saharan dust source activation frequency map derived from MSG-SEVIRI IR-Channels, Geophysical Research Letter, 34, 18803, doi: 10.1029/2007GL030168.

Schepanski, K., Tegen, I., and Macke, A.: Comparison of satellite based observations of Saharan dust source areas, Remote Sensing of Environment, 123, 90-97, dpi:10.1016/j.rse.2012.03.019, 2012

Seager R, et al. (2007) Model projections of an imminent transition to a more arid climate in southwestern North America. *Science 316:1181–1184.*

Slanina, J., Baard, J.H., Zijp, W.L., 1983. Tracing the sources of chemical composition of precipitation by cluster analysis. Water, Air & Soil Pollution 20, 41–45.

Sorooshian, A., A. Wonaschütz, E. G. Jarjour, B. I. Hashimoto, B. A. Schichtel, and E. A. Betterton (2011), An aerosol climatology for a rapidly growing arid region (southern Arizona): Major aerosol species and remotely sensed aerosol properties, *J. Geophys. Res.*, 116, D19205, doi:10.1029/2011JD016197.

Schutz, L. and M. Sebert, 1987. Mineral aerosols and source identification. Journal of Aerosol Science, 18(1), 1-10.

Sun, Y., Zhuang, G., Yuan, H., Zhang, X., Guo, J., 2004. Characteristics and sources of 2002 super dust storm in Beijing. Chinese Science Bulletin 49(7), 698-705.

Tanré, D., Y.J. Kaufman, M. Herman, and S. Mattoo, Remote sensing of aerosol properties over oceans using the MODIS/EOS spectral radiances., J. Geophys. Res., 102, 16,971– 16,988, 1997.

Taylor, S.R. and S.M. McLennan 1985. The Continental Crust: Its Composition and Evolution, 312p., Blackwell, Cambridge, Massachusetts.

Tegen, I., and R. Miller (1998), A general circulation model study on the interannual variability of soil dust aerosol. *J. Geophys. Res.*, 103 (D20)25,975-25,995, doi: 10.1029/98JD023454.

Tong, D.Q., D. Kang, V.P. Aneja, J.D. Ray, 2005. Reactive nitrogen oxides in the southeast United States national parks: source identification, origin, and process budget. *Atmospheric Environment* 39 (2005) 315–327.

Van Curen, R.A., T.A. Cahill, Asian aerosols in North America: frequency and concentration of fine dust, *J. Geophys. Res., 107*, D24, doi: 10.1029/2002JD002204, 2002.

Wang, Y., Zhuang, G., Sun, Y., An, Z.., 2005. Water-soluble part of the aerosol in the dust storm season—evidence of the mixing between mineral and pollution aerosols. Atmospheric Environment 39, 7020–7029.

Wells, K. C., M. Witek, P. Flatau, S. M. Kreidenweis, and D. L. Westphal (2007), An analysis of seasonal surface dust aerosol concentrations in the western U.S. (2001–2004): Observations and model predictions, *Atmos. Environ.*, 41, 6585–6597, doi:10.1016/j.atmosenv.2007.04.034.

Zhang, X. Y., S. L. Gong, Z. X. Shen, F. M. Mei, X. X. Xi, L. C. Liu, Z. J. Zhou, D. Wang, Y. Q. Wang, and Y. Cheng, Characterization of soil dust aerosol in China and its transport and distribution during 2001 ACE-Asia: 1. Network observations, J. Geophys. Res., 108(D9), 4261, doi:10.1029/2002JD002632, 2003.

Table 1. Identified local dust events from the IMPROVE monitoring network from 2000 to 2007. The concentrations and ratios listed in the table represent the mean values if there is more than one identified dust episode.

Site	**SiteID**	**Longitude**	**Latitude**	**PM10** (mg/m3)	**PM2.5** (mg/m3)	**PM2.5/PM10 Ratio**	**Local Dust Events** (YYMMDD)
1	BOAP1	-106.85	33.87	42.44	6.99	0.16	11016
2	GICL1	-108.24	33.22	35.59	7.71	0.22	70328
3	SACR1	-104.4	33.46	72.15	15.95	0.22	010410, 010925, 030415, 030602, 030605, 031226, 050311, 051203, 060312, 060619, 060622, 071114
4	WHIT1	-105.54	33.47	89.55	20.42	0.23	020426, 060216
5	BIBE1	-103.18	29.3	53.25	12.36	0.24	000322, 000422, 000921, 010209, 011124, 020210, 020309, 020312, 020330, 020402, 020616, 021110, 030328, 030406, 030415, 051127
6	GUMO1	-104.81	31.83	73.2	15.63	0.22	000422, 000517, 010422, 010603, 010624, 010715, 011016, 020309, 020420, 020502, 020511, 020526, 020610, 020613, 020619, 030202, 030304, 030415, 030418, 030515, 030723, 031208, 031226, 040608, 051127, 060318, 070223
7	CHIR1	-109.39	32.01	73.34	17.05	0.24	000408, 011109, 030521, 030717, 051127, 060601, 060716, 061222, 070328
8	IKBA1	-111.68	34.34	62.53	18.76	0.29	010621, 020514, 030515, 030521, 030530, 030726, 040903, 070412, 070720
9	QUVA1	-111.29	33.29	61.2	13.64	0.22	011016, 020426, 020514, 030202, 030515, 030521, 030617, 030620, 030714, 030717, 030909, 041021, 060216, 060414, 060716, 060725, 070418, 070708, 071018
10	SAGU1	-110.74	32.17	57.79	18.13	0.31	011109, 030521, 030717, 060625, 070328, 070412
11	SAWE1	-111.22	32.25	75.59	20.23	0.25	011109, 030521, 030711, 030717, 030909, 070328, 070412, 070415, 070521
12	SIAN1	-110.94	34.09	59.6	17.22	0.3	011016, 030515, 030530, 070412, 060716
13	TONT1	-111.11	33.65	61.6	13.89	0.23	060716, 070412, 070708, 070720, 071006
14	PEFO1	-109.769	35.07	55.4	13	0.24	030509, 050404,050419
15	AGTI1	-116.97	33.46	72.46	13.69	0.19	010817, 021125, 030106, 070412
16	DEVA1	-116.85	36.51	63.95	12	0.19	020508, 020511, 020520, 040903, 061228
17	DOME1	-118.14	35.73	65.6	6.86	0.1	31030
18	JOSH1	-116.39	34.07	69.56	15.97	0.27	000812, 011001, 020731, 030819, 050802, 060625
19	SAGA1	-118.03	34.3	45.12	6.43	0.14	21002
20	SAGO1	-116.91	34.19	71.09	10.97	0.16	021125, 070412, 070521
21	SEQU1	-118.83	36.49	78.61	10.06	0.16	020710, 031030
22	HOOV1	-119.18	38.09	149.29	45.76	0.31	20228
23	GRBA1	-114.22	39.01	104.62	18.85	0.18	20228
24	WARI1	-118.82	38.95	70.39	12.85	0.19	030921, 040310, 040903, 050916, 050922
25	INGA1	-112.13	36.08	107.08	32.39	0.3	70720
26	GRSA1	-105.52	37.72	51.28	11.1	0.23	000517, 020511, 030503, 050603
27	MEVE1	-108.49	37.2	65.2	13.68	0.22	030202, 030415, 050419
28	DOUG1	-109.54	31.35	81.27	21.2	0.26	070328 ,071108
29	PHOE1	-112.1	33.5	76.82	15.93	0.21	011016, 020511, 020722, 020917, 030202, 030515, 030530, 030714, 030717, 030909, 060405, 060414, 060625, 070412, 070720
30	FRES1	-119.77	36.78	88.88	16.65	0.19	040915, 060914, 060929, 061026, 070912

Table 2. Comparisons of three simplified dust identification methods to the full method proposed in this study. Here the dust records identified by the full method are used as reference data to calculate hits and false alarms.

Method	**Hits** [d]	**False Alarms** [e]	**Hit Rate** [f]	**False Alarm Ratio** [g]
Simplified Method I [a]	49	381	27%	68%
Simplified Approach II [b]	24	86	13%	16%
Ganor Approach [c]	38	42	21%	29%

a. Method I uses two threshold values (PM_{10} > 40 μg/m^3, and $PM_{2.5}/PM_{10}$ ratio < 0.35) to identify dust events;
b. Method II is similar to that of Method I, except that the $PM_{2.5}/PM_{10}$ threshold value is set to be 0.20;
c. The Ganor method (revised from Ganor et al., 2009) uses 24-hour PM_{10} concentration > 100 μg/m^3 as the sole criteria.
d. Hits are the number of dust records identified by both the simple method and the full method;
e. False alarms are the dust records selected by the simple method, but not by the full method.
f. Hit Rate is the percentage of "true" dust events identified by the simple method to all events by the full method,
g. False Alarm Ratio is the percentage of "false" events (i.e., not considered local dust events by the full method) to all events selected by the simple methods.

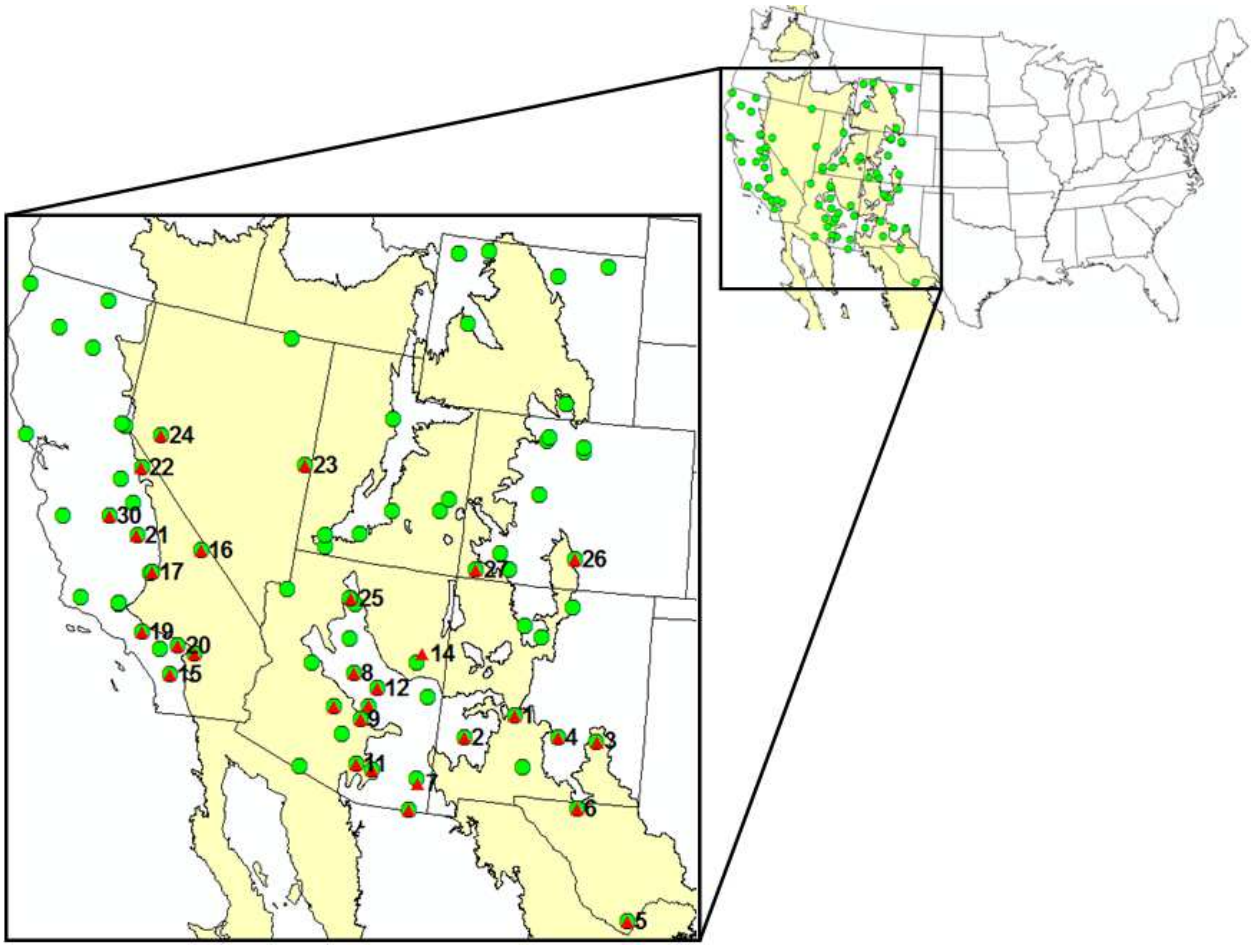

Figure 1. Locations of the 68 selected IMPROVE monitors from which the aerosol observation data are used in this study. The 30 sites (marked in red) indicate the locations where at least one local dust storm has been identified between 2000 and 2007 using the approach proposed in this work. The background is the area classified as arid or semi-arid land.

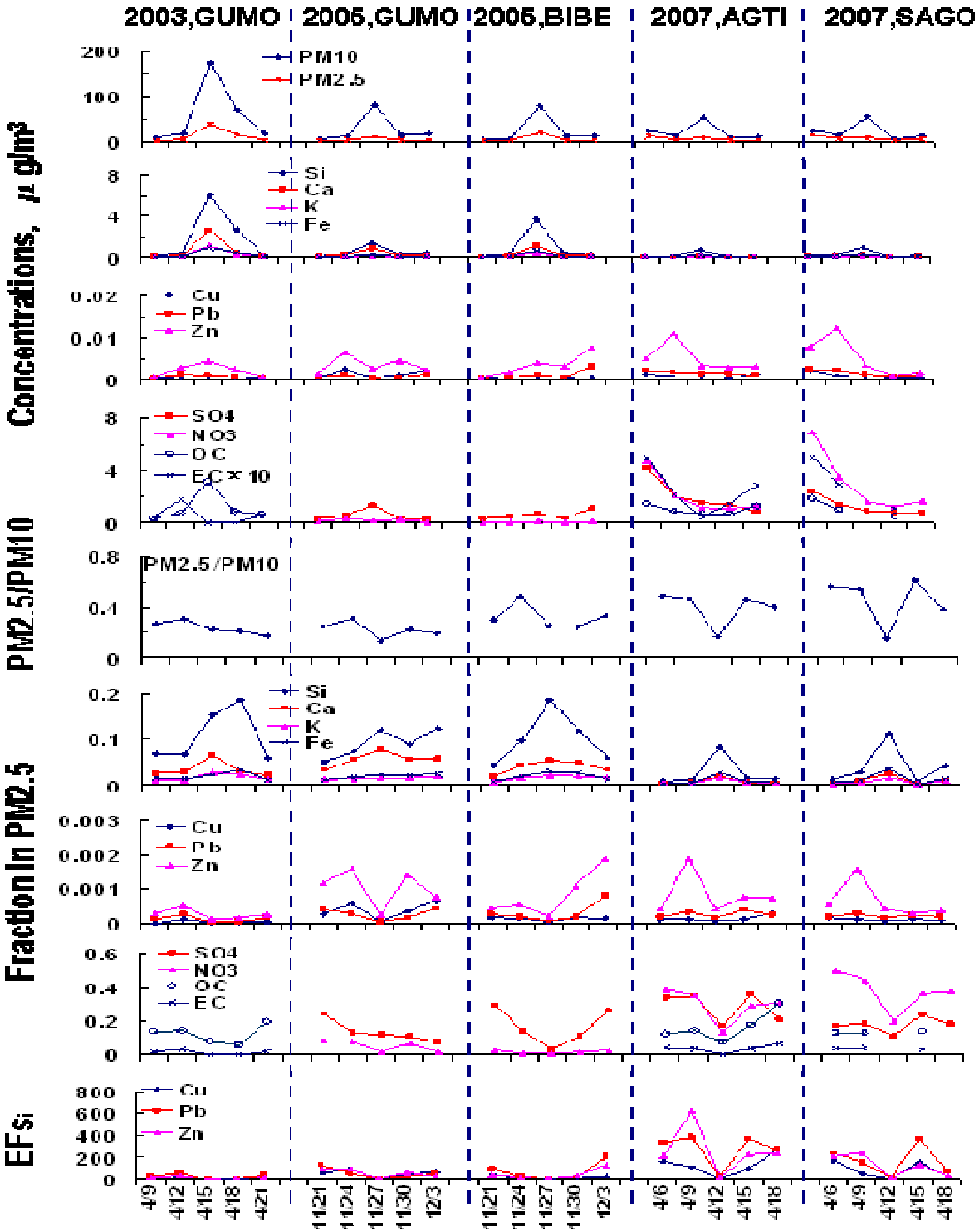

Figure2. Variations of PM_{10}, $PM_{2.5}$ and chemical components of $PM_{2.5}$ at the BIBE1, GUMO1, AGTI1 and SAGO1 sites during, before and after three dust storms. These dust events have been pinpointed by MODIS satellite data. "Fraction in PM2.5" indicates the fraction of the concerned aerosol component to total $PM_{2.5}$ mass, and EF_{Si} indicates the enrichment factors of concerned species using Si as the referent element.

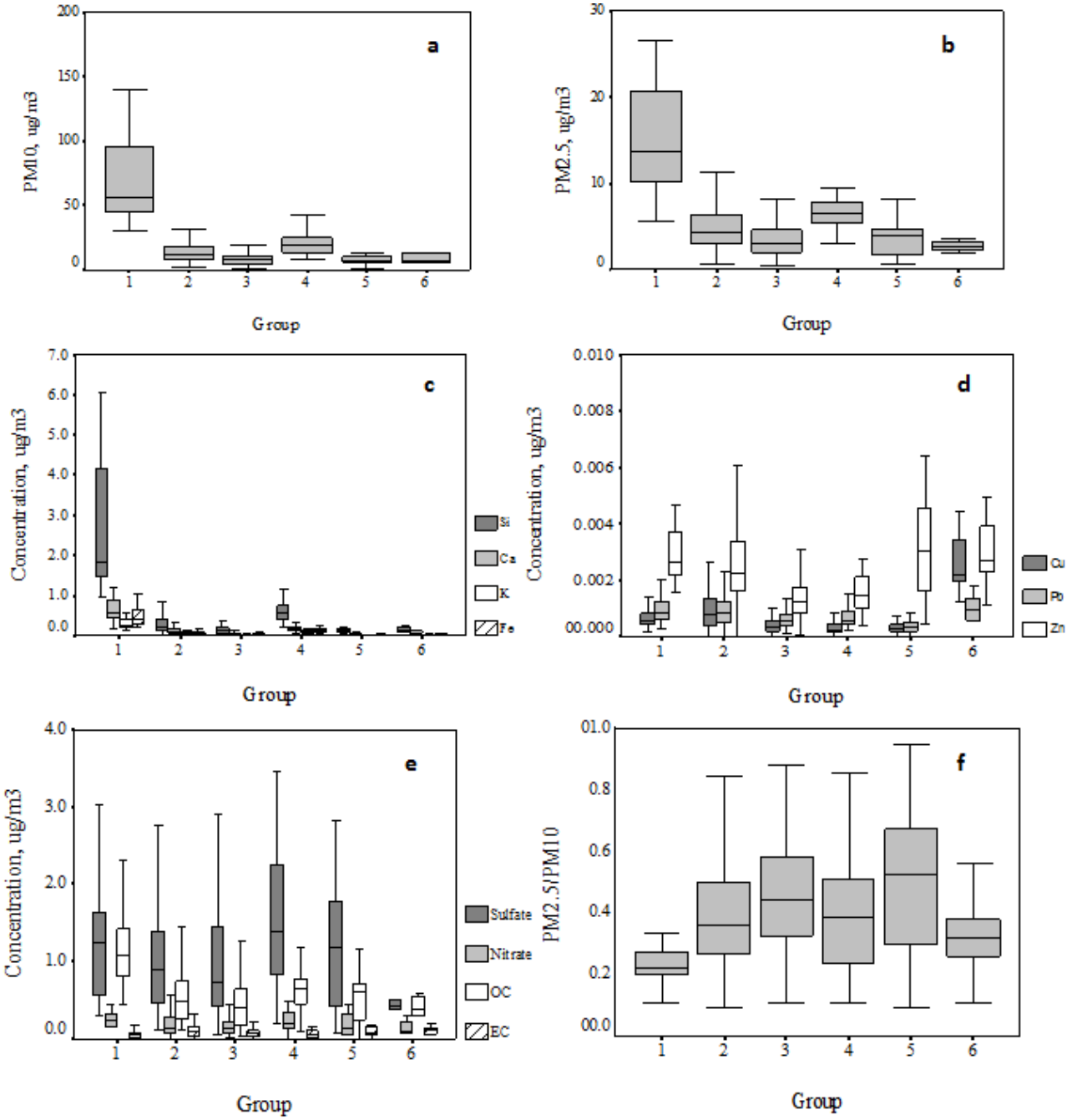

Figure 3. Physical and chemical characteristics of aerosol samples in different clusters as generated by the hierarchical cluster analysis of all IMPROVE observation data from 2000 to 2007 at the GUMO1 site: (a) PM_{10} mass; (b) $PM_{2.5}$ mass; (c) crustal elements, Si, Ca, K, Fe; (d) anthropogenic trace elements, Cu, Zn, Pb; (e) Sulfate, Nitrate, OC and EC; and (f) $PM_{2.5}/PM_{10}$ ratio. The bottom and top edges of the box indicates the 25th and 75th percentile and the line in the box indicates the 50%. Group 1 was identified as the local dust group.

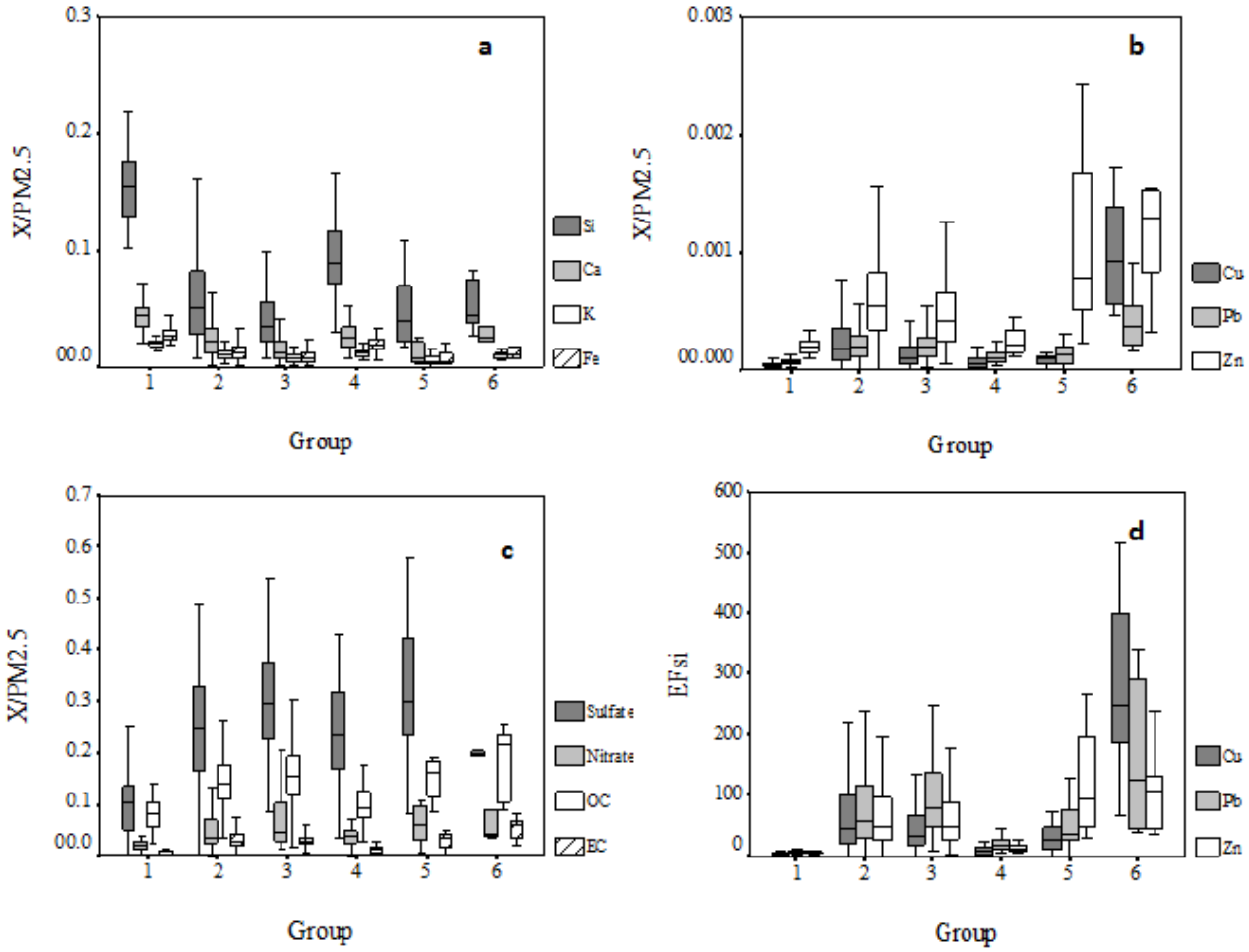

Figure 4. Physical and chemical characteristics of aerosol samples in different clusters as generated by the hierarchical cluster analysis of all IMPROVE observation data from 2000 to 2007 at the GUMO1 site (continued): (a) mass fractions of Si, Ca, K, and Fe in in $PM_{2.5}$; (b) mass fractions of Cu, Zn, and Pb in $PM_{2.5}$; (c) mass fractions of Sulfate, Nitrate, OC and EC in $PM_{2.5}$; (d) enrichment factors of Cu, Zn and Pb using Si as the reference element between different groups classified by cluster analysis. The bottom and top edges of the box indicates the 25th and 75th percentile and the line in the box indicates the 50%. Group 1 was identified as the local dust group.

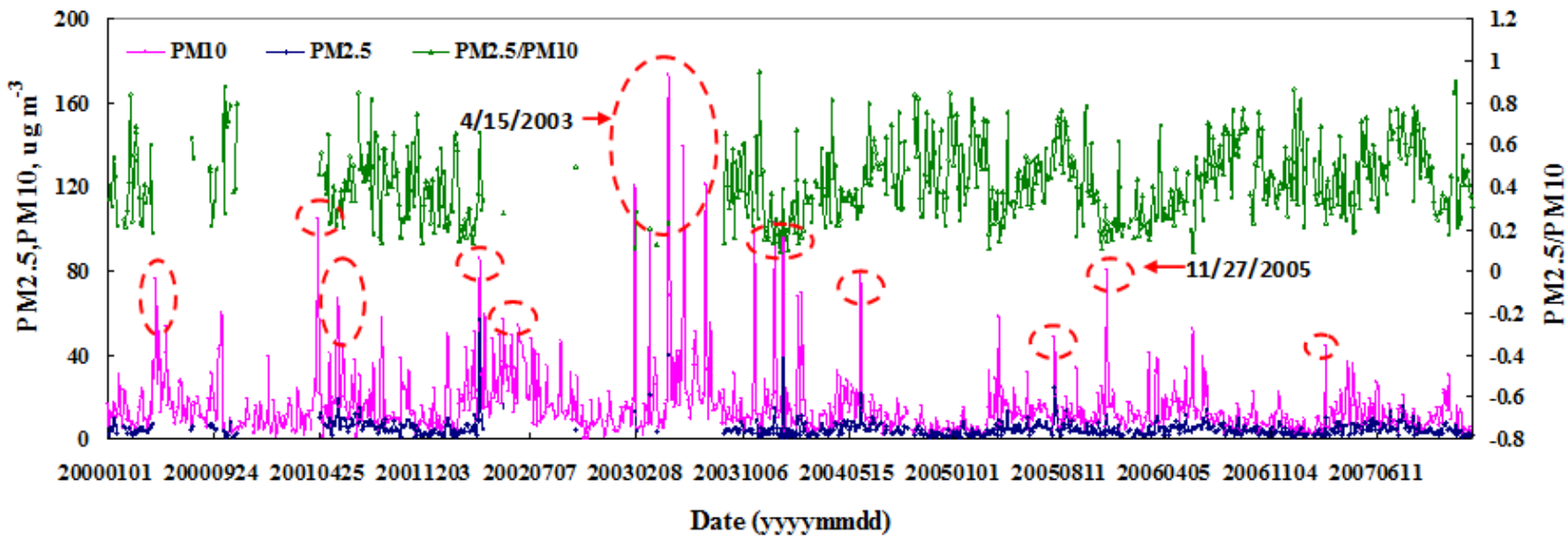

Figure 5. Time series of PM_{10} and $PM_{2.5}$ mass concentrations and their ratio at the Guadalupe Mountains National Park, TX (GUMO1) site between 2000 and 2007. Red circles indicate local dust events identified using the dust identification approach. The approach has effectively captured all satellite pinpointed dust events, including the April 15, 2003 storm and the November 27, 2005 storm.

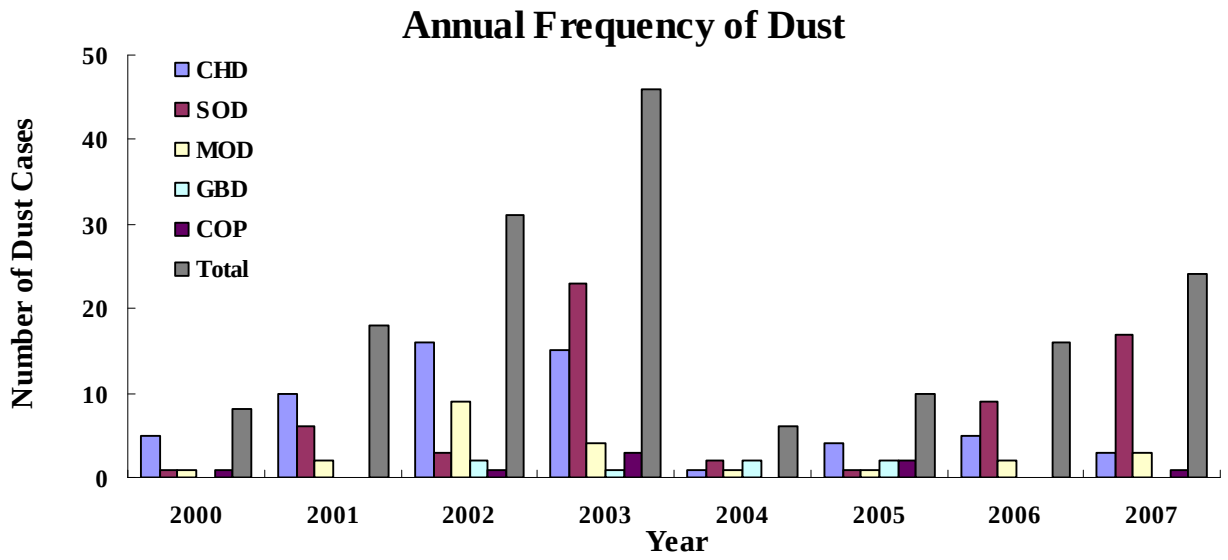

Figure 6. The annual frequency of local dust cases from 2000 to 2007 in the five dust source regions, namely, the Chihuahuan Desert (CHD), the Sonoran Desert (SOD), the Mojave Desert (MOD), the Great Basin Desert (GBD) and the Colorado Plateau (COP).

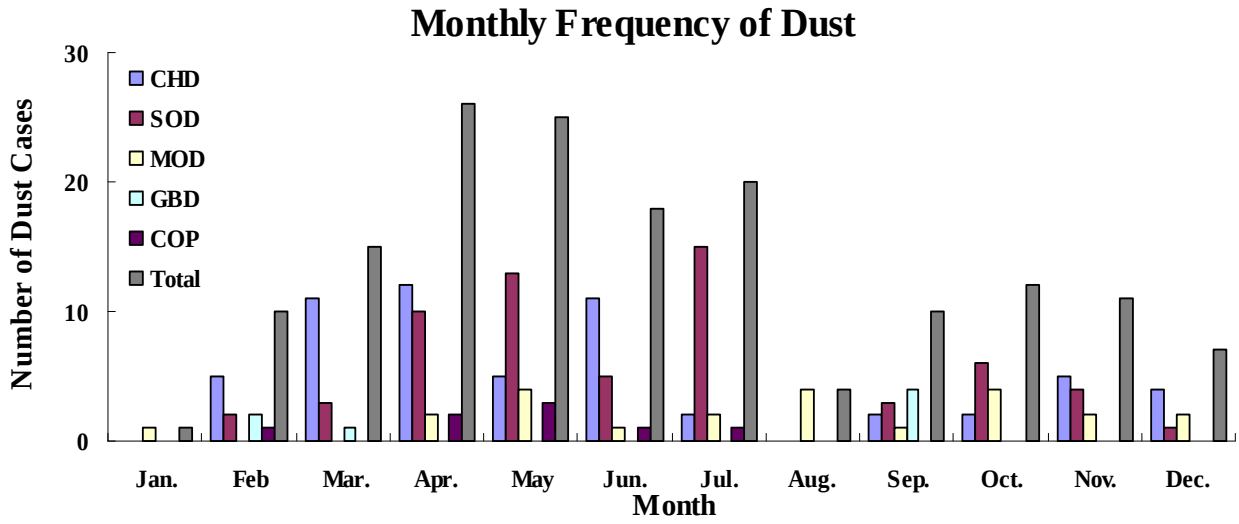

Figure 7. The monthly frequency of local dust cases from 2000 to 2007 in the five dust source regions, namely, the Chihuahuan Desert (CHD), the Sonoran Desert (SOD), the Mojave Desert (MOD), the Great Basin Desert (GBD) and the Colorado Plateau (COP).

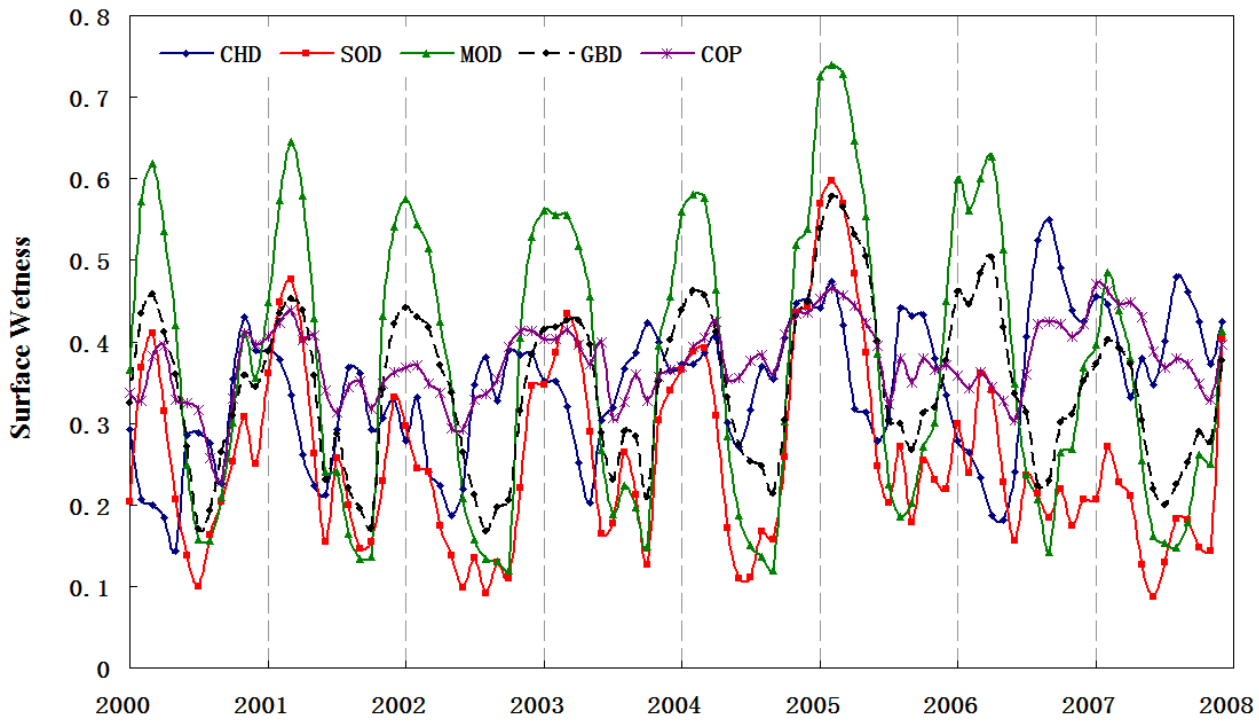

Figure 8. Monthly variations of surface wetness over five dust source regions during the study period. The surface wetness is derived from the NASA Modern Era Retrospective-analysis for Research and Application (MERRA) dataset. Five dust regions include the Chihuahuan Desert (CHD), the Sonoran Desert (SOD), the Mojave Desert (MOD), the Great Basin Desert (GBD) and the Colorado Plateau (COP).